Shape and Time Distortion Loss for Training Deep Time Series Forecasting Models

Vincent Le Guen [1,2]
vincent.le-guen@edf.fr

Nicolas Thome [2]
nicolas.thome@cnam.fr

(1) EDF R&D
6 quai Watier, 78401 Chatou, France

(2) CEDRIC, Conservatoire National des Arts et Métiers
292 rue Saint-Martin, 75003 Paris, France

Abstract

This paper addresses the problem of time series forecasting for non-stationary signals and multiple future steps prediction. To handle this challenging task, we introduce DILATE (DIstortion Loss including shApe and TimE), a new objective function for training deep neural networks. DILATE aims at accurately predicting sudden changes, and explicitly incorporates two terms supporting precise shape and temporal change detection. We introduce a differentiable loss function suitable for training deep neural nets, and provide a custom back-prop implementation for speeding up optimization. We also introduce a variant of DILATE, which provides a smooth generalization of temporally-constrained Dynamic Time Warping (DTW). Experiments carried out on various non-stationary datasets reveal the very good behaviour of DILATE compared to models trained with the standard Mean Squared Error (MSE) loss function, and also to DTW and variants. DILATE is also agnostic to the choice of the model, and we highlight its benefit for training fully connected networks as well as specialized recurrent architectures, showing its capacity to improve over state-of-the-art trajectory forecasting approaches.

1 Introduction

Time series forecasting [6] consists in analyzing the dynamics and correlations between historical data for predicting future behavior. In one-step prediction problems [39, 30], future prediction reduces to a single scalar value. This is in sharp contrast with multi-step time series prediction [49, 2, 48], which consists in predicting a complete trajectory of future data at a rather long temporal extent. Multi-step forecasting thus requires to accurately describe time series evolution.

This work focuses on multi-step forecasting problems for non-stationary signals, *i.e.* when future data cannot only be inferred from the past periodicity, and when abrupt changes of regime can occur. This includes important and diverse application fields, *e.g.* regulating electricity consumption [63, 36], predicting sharp discontinuities in renewable energy production [23] or in traffic flow [35, 34], electrocardiogram (ECG) analysis [9], stock markets prediction [14], *etc*.

Deep learning is an appealing solution for this multi-step and non-stationary prediction problem, due to the ability of deep neural networks to model complex nonlinear time dependencies. Many approaches have recently been proposed, mostly relying on the design of specific one-step ahead

33rd Conference on Neural Information Processing Systems (NeurIPS 2019), Vancouver, Canada.

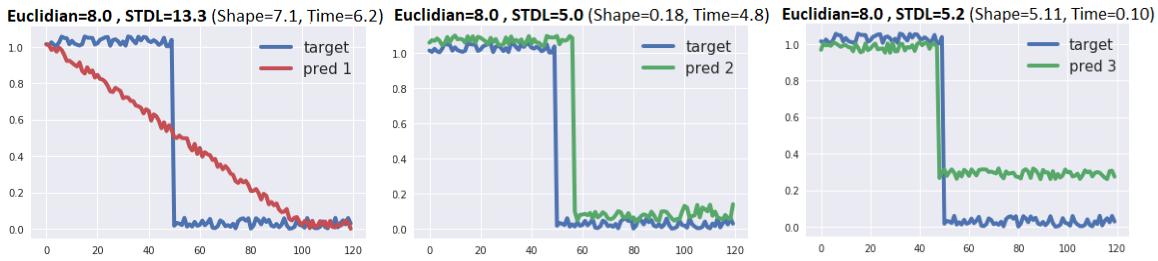

(a) Non informative prediction (b) Correct shape, time delay (c) Correct time, inaccurate shape

Figure 1: Limitation of the euclidean (MSE) loss: when predicting a sudden change (target blue step function), the 3 predictions (a), (b) and (c) have similar MSE but very different forecasting skills. In contrast, the DILATE loss proposed in this work, which disentangles shape and temporal decay terms, supports predictions (b) and (c) over prediction (a) that does not capture the sharp change of regime.

architectures recursively applied for multi-step [24, 26, 7, 5], on direct multi-step models [3] such as Sequence To Sequence [34, 60, 57, 61] or State Space Models for probabilistic forecasts [44, 40].

Regarding training, the huge majority of methods use the Mean Squared Error (MSE) or its variants (MAE, *etc*) as loss functions. However, relying on MSE may arguably be inadequate in our context, as illustrated in Fig 1. Here, the target ground truth prediction is a step function (in blue), and we present three predictions, shown in Fig 1(a), (b), and (c), which have a similar MSE loss compared to the target, but very different forecasting skills. Prediction (a) is not adequate for regulation purposes since it doesn't capture the sharp drop to come. Predictions (b) and (c) much better reflect the change of regime since the sharp drop is indeed anticipated, although with a slight delay (b) or with a slight inaccurate amplitude (c).

This paper introduces DILATE (DIstortion Loss including shApe and TimE), a new objective function for training deep neural networks in the context of multi-step and non-stationary time series forecasting. DILATE explicitly disentangles into two terms the penalization related to the shape and the temporal localization errors of change detection (section 3). The behaviour of DILATE is shown in Fig 1: whereas the values of our proposed shape and temporal losses are large in Fig 1(a), the shape (resp. temporal) term is small in Fig 1(b) (resp. Fig 1(c)). DILATE combines shape and temporal terms, and is consequently able to output a much smaller loss for predictions (b) and (c) than for (a), as expected.

To train deep neural nets with DILATE, we derive a differentiable loss function for both shape and temporal terms (section 3.1), and an efficient and custom back-prop implementation for speeding up optimization (section 3.2). We also introduce a variant of DILATE, which provides a smooth generalization of temporally-constrained Dynamic Time Warping (DTW) metrics [43, 28]. Experiments carried out on several synthetic and real non-stationary datasets reveal that models trained with DILATE significantly outperform models trained with the MSE loss function when evaluated with shape and temporal distortion metrics, while DILATE maintains very good performance when evaluated with MSE. Finally, we show that DILATE can be used with various network architectures and can outperform on shape and time metrics state-of-the-art models specifically designed for multi-step and non-stationary forecasting.

2 Related work

Time series forecasting Traditional methods for time series forecasting include linear auto-regressive models, such as the ARIMA model [6], and Exponential Smoothing [27], which both fall into the broad category of linear State Space Models (SSMs) [17]. These methods handle linear dynamics and stationary time series (or made stationary by temporal differences). However the stationarity assumption is not satisfied for many real world time series that can present abrupt changes of distribution. Since, Recurrent Neural Networks (RNNs) and variants such as Long Short Term Memory Networks (LSTMs) [25] have become popular due to their automatic feature extraction abilities, complex patterns and long term dependencies modeling. In the era of deep learning, much effort has been recently devoted to tackle multivariate time series forecasting with a huge number of input

series [31], by leveraging attention mechanisms [30, 39, 50, 12] or tensor factorizations [60, 58, 46] for capturing shared information between series. Another current trend is to combine deep learning and State Space Models for modeling uncertainty [45, 44, 40, 56]. In this paper we focus on deterministic multi-step forecasting. To this end, the most common approach is to apply recursively a one-step ahead trained model. Although mono-step learned models can be adapted and improved for the multi-step setting [55], a thorough comparison of the different multi-step strategies [48] has recommended the direct multi-horizon strategy. Of particular interest in this category are Sequence To Sequence (Seq2Seq) RNNs models [1] [44, 31, 60, 57, 19] which achieved great success in machine translation. Theoretical generalization bounds for Seq2Seq forecasting were derived with an additional discrepancy term quantifying the non-stationarity of time series [29]. Following the success of WaveNet for audio generation [53], Convolutional Neural Networks with dilation have become a popular alternative for time series forecasting [5]. The self-attention Transformer architecture [54] was also lately investigated for accessing long-range context regardless of distance [32]. We highlight that our proposed loss function can be used for training any direct multi-step deep architecture.

Evaluation and training metrics The largely dominant loss function to train and evaluate deep models is the MAE, MSE and its variants (SMAPE, etc). Metrics reflecting shape and temporal localization exist: Dynamic Time Warping [43] for shape ; timing errors can be casted as a detection problem by computing Precision and Recall scores after segmenting series by Change Point Detection [8, 33], or by computing the Hausdorff distance between two sets of change points [22, 51]. For assessing the detection of ramps in wind and solar energy forecasting, specific algorithms were designed: for shape, the ramp score [18, 52] based on a piecewise linear approximation of the derivatives of time series; for temporal error estimation, the Temporal Distortion Index (TDI) [20, 52]. However, these evaluation metrics are not differentiable, making them unusable as loss functions for training deep neural networks. The impossibility to directly optimize the appropriate (often non-differentiable) evaluation metric for a given task has bolstered efforts to design good surrogate losses in various domains, for example in ranking [15, 62] or computer vision [38, 59].

Recently, some attempts have been made to train deep neural networks based on alternatives to MSE, especially based on a smooth approximation of the Dynamic time warping (DTW) [13, 37, 1]. Training DNNs with a DTW loss enables to focus on the shape error between two signals. However, since DTW is by design invariant to elastic distortions, it completely ignores the temporal localization of the change. In our context of sharp change detection, both shape and temporal distortions are crucial to provide an adequate forecast. A differentiable timing error loss function based on DTW on the event (binary) space was proposed in [41] ; however it is only applicable for predicting binary time series. This paper specifically focuses on designing a loss function able to disentangle shape and temporal delay terms for training deep neural networks on real world time series.

3 Training Deep Neural Networks with DILATE

Our proposed framework for multi-step forecasting is depicted in Figure 2. During training, we consider a set of N input time series $\mathcal{A} = \{\mathbf{x}_i\}_{i\in\{1:N\}}$. For each input example of length n, *i.e.* $\mathbf{x}_i = (\mathbf{x}_i^1, ..., \mathbf{x}_i^n) \in \mathbb{R}^{p\times n}$, a forecasting model such as a neural network predicts the future k-step ahead trajectory $\hat{\mathbf{y}}_i = (\hat{\mathbf{y}}_i^1, ..., \hat{\mathbf{y}}_i^k) \in \mathbb{R}^{d\times k}$. Our DILATE objective function, which compares this prediction $\hat{\mathbf{y}}_i$ with the actual ground truth future trajectory $\overset{*}{\mathbf{y}}_i = (\overset{*}{\mathbf{y}}_i{}^1, ..., \overset{*}{\mathbf{y}}_i{}^k)$ of length k, is composed of two terms balanced by the hyperparameter $\alpha \in [0, 1]$:

$$\mathcal{L}_{DILATE}(\hat{\mathbf{y}}_i, \overset{*}{\mathbf{y}}_i) = \alpha\, \mathcal{L}_{shape}(\hat{\mathbf{y}}_i, \overset{*}{\mathbf{y}}_i) + (1-\alpha)\, \mathcal{L}_{temporal}(\hat{\mathbf{y}}_i, \overset{*}{\mathbf{y}}_i) \tag{1}$$

Notations and definitions Both our shape $\mathcal{L}_{shape}(\hat{\mathbf{y}}_i, \overset{*}{\mathbf{y}}_i)$ and temporal $\mathcal{L}_{temporal}(\hat{\mathbf{y}}_i, \overset{*}{\mathbf{y}}_i)$ distortions terms are based on the alignment between predicted $\hat{\mathbf{y}}_i \in \mathbb{R}^{d\times k}$ and ground truth $\overset{*}{\mathbf{y}}_i \in \mathbb{R}^{d\times k}$ time series. We define a warping path as a binary matrix $\mathbf{A} \subset \{0, 1\}^{k\times k}$ with $A_{h,j} = 1$ if $\hat{\mathbf{y}}_i^h$ is associated to $\overset{*}{\mathbf{y}}_i{}^j$, and 0 otherwise. The set of all valid warping paths connecting the endpoints $(1, 1)$ to (k, k)

[1] A Seq2Seq architecture was the winner of a 2017 Kaggle competition on multi-step time series forecasting (https://www.kaggle.com/c/web-traffic-time-series-forecasting)

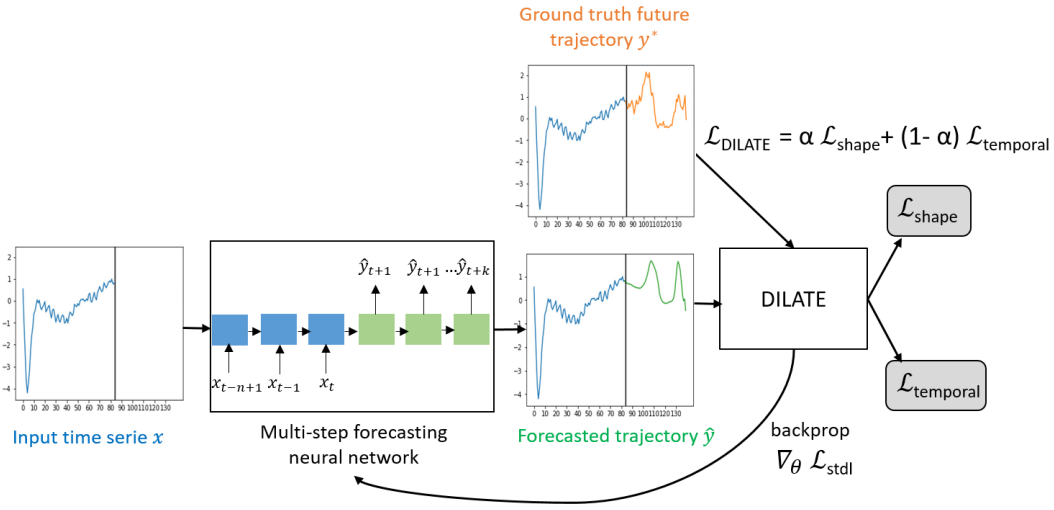

Figure 2: Our proposed framework for training deep forecasting models.

with the authorized moves $\rightarrow, \downarrow, \searrow$ (step condition) is noted $\mathcal{A}_{k,k}$. Let $\mathbf{\Delta}(\hat{\mathbf{y}}_i, \overset{*}{\mathbf{y}}_i) := [\delta(\hat{\mathbf{y}}_i^h, \overset{*}{\mathbf{y}}_i^{\mathrm{j}})]_{h,j}$ be the pairwise cost matrix, where δ is a given dissimilarity between $\hat{\mathbf{y}}_i^h$ and $\overset{*}{\mathbf{y}}_i^{\mathrm{j}}$, *e.g.* the euclidean distance.

3.1 Shape and temporal terms

Shape term Our shape loss function is based on the Dynamic Time Warping (DTW) [43], which corresponds to the following optimization problem: $DTW(\hat{\mathbf{y}}_i, \overset{*}{\mathbf{y}}_i) = \min_{\mathbf{A} \in \mathcal{A}_{k,k}} \left\langle \mathbf{A}, \mathbf{\Delta}(\hat{\mathbf{y}}_i, \overset{*}{\mathbf{y}}_i) \right\rangle$. $\mathbf{A}^* = \underset{A \in \mathcal{A}_{k,k}}{\arg\min} \left\langle \mathbf{A}, \mathbf{\Delta}(\hat{\mathbf{y}}_i, \overset{*}{\mathbf{y}}_i) \right\rangle$ is the optimal association (path) between $\hat{\mathbf{y}}_i$ and $\overset{*}{\mathbf{y}}_i$. By temporally aligning the predicted $\hat{\mathbf{y}}_i$ and ground truth $\overset{*}{\mathbf{y}}_i$ time series, the DTW loss focuses on the structural shape dissimilarity between signals. The DTW, however, is known to be non-differentiable. We use the smooth min operator $\min_\gamma(a_1, ..., a_n) = -\gamma \log(\sum_i^n \exp(-a_i/\gamma))$ with $\gamma > 0$ proposed in [13] to define our differentiable shape term $\mathcal{L}_{shape}$:

$$\mathcal{L}_{shape}(\hat{\mathbf{y}}_i, \overset{*}{\mathbf{y}}_i) = DTW_\gamma(\hat{\mathbf{y}}_i, \overset{*}{\mathbf{y}}_i) := -\gamma \log \left(\sum_{\mathbf{A} \in \mathcal{A}_{k,k}} \exp \left(-\frac{\left\langle \mathbf{A}, \mathbf{\Delta}(\hat{\mathbf{y}}_i, \overset{*}{\mathbf{y}}_i) \right\rangle}{\gamma} \right) \right) \tag{2}$$

Temporal term Our second term $\mathcal{L}_{temporal}$ in Eq (1) aims at penalizing temporal distortions between $\hat{\mathbf{y}}_i$ and $\overset{*}{\mathbf{y}}_i$. Our analysis is based on the optimal DTW path $\mathbf{A}^*$ between $\hat{\mathbf{y}}_i$ and $\overset{*}{\mathbf{y}}_i$. $\mathbf{A}^*$ is used to register both time series when computing DTW and provide a time-distortion invariant loss. Here, we analyze the form of $\mathbf{A}^*$ to compute the temporal distortions between $\hat{\mathbf{y}}_i$ and $\overset{*}{\mathbf{y}}_i$. More precisely, our loss function is inspired from computing the Time Distortion Index (TDI) for temporal misalignment estimation [20, 52], which basically consists in computing the deviation between the optimal DTW path $\mathbf{A}^*$ and the first diagonal. We first rewrite a generalized TDI loss function with our notations:

$$TDI(\hat{\mathbf{y}}_i, \overset{*}{\mathbf{y}}_i) = \langle \mathbf{A}^*, \mathbf{\Omega} \rangle = \left\langle \underset{\mathbf{A} \in \mathcal{A}_{k,k}}{\arg\min} \left\langle \mathbf{A}, \mathbf{\Delta}(\hat{\mathbf{y}}_i, \overset{*}{\mathbf{y}}_i) \right\rangle, \mathbf{\Omega} \right\rangle \tag{3}$$

where $\mathbf{\Omega}$ is a square matrix of size $k \times k$ penalizing each element $\hat{\mathbf{y}}_i^h$ being associated to an $\overset{*}{\mathbf{y}}_i^j$, for $h \neq j$. In our experiments we choose a squared penalization, *e.g.* $\mathbf{\Omega}(h, j) = \frac{1}{k^2}(h - j)^2$, but other

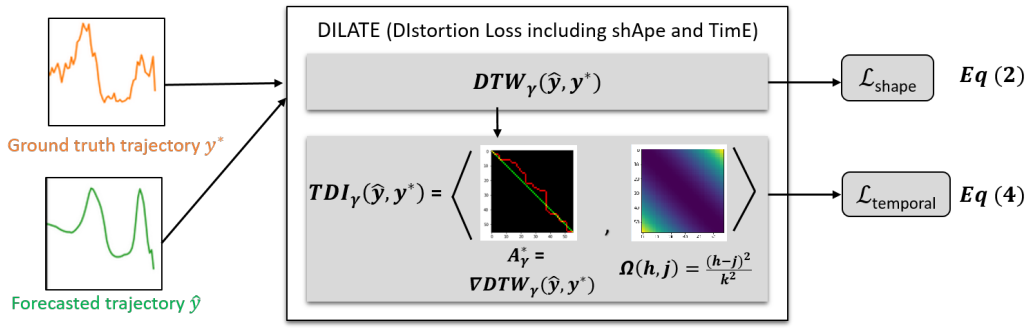

Figure 3: DILATE loss computation for separating the shape and temporal errors.

variants could be used. Note that *prior* knowledge can also be incorporated in the $\mathbf{\Omega}$ matrix structure, *e.g.* to penalize more heavily late than early predictions (and *vice versa*).

The TDI loss function in Eq (3) is still non-differentiable. Here, we cannot directly use the same smoothing technique that for defining DTW_γ in Eq (2), since the minimization involves two different quantities $\mathbf{\Omega}$ and $\mathbf{\Delta}$. Since the optimal path $\mathbf{A}^*$ is itself non-differentiable, we use the fact that $\mathbf{A}^* = \nabla_\Delta DTW(\hat{\mathbf{y}}_i, \overset{*}{\mathbf{y}}_i)$ to define a smooth approximation $\mathbf{A}^*_\gamma$ of the $\arg\min$ operator, *i.e.* :

$\mathbf{A}^*_\gamma = \nabla_\Delta DTW_\gamma(\hat{\mathbf{y}}_i, \overset{*}{\mathbf{y}}_i) = 1/Z \sum_{\mathbf{A} \in \mathcal{A}_{k,k}} \mathbf{A} \exp^{-\frac{\left\langle \mathbf{A}, \mathbf{\Delta}(\hat{\mathbf{y}}_i, \overset{*}{\mathbf{y}}_i) \right\rangle}{\gamma}}$, with $Z = \sum_{\mathbf{A} \in \mathcal{A}_{k,k}} \exp^{-\frac{\left\langle \mathbf{A}, \mathbf{\Delta}(\hat{\mathbf{y}}_i, \overset{*}{\mathbf{y}}_i) \right\rangle}{\gamma}}$ being the partition function. Based on $\mathbf{A}^*_\gamma$, we obtain our smoothed temporal loss from Eq (3):

$$\mathcal{L}_{temporal}(\hat{\mathbf{y}}_i, \overset{*}{\mathbf{y}}_i) := \left\langle \mathbf{A}^*_\gamma, \mathbf{\Omega} \right\rangle = \frac{1}{Z} \sum_{\mathbf{A} \in \mathcal{A}_{k,k}} \langle \mathbf{A}, \mathbf{\Omega} \rangle \exp^{-\frac{\left\langle \mathbf{A}, \mathbf{\Delta}(\hat{\mathbf{y}}_i, \overset{*}{\mathbf{y}}_i) \right\rangle}{\gamma}} \tag{4}$$

3.2 DILATE Efficient Forward and Backward Implementation

The direct computation of our shape and temporal losses in Eq (2) and Eq (4) is intractable, due to the cardinal of $\mathcal{A}_{k,k}$, which exponentially grows with k. We provide a careful implementation of the forward and backward passes in order to make learning efficient.

Shape loss Regarding $\mathcal{L}_{shape}$, we rely on [13] to efficiently compute the forward pass with a variant of the Bellmann dynamic programming approach [4]. For the backward pass, we implement the recursion proposed in [13] in a custom Pytorch loss. This implementation is much more efficient than relying on vanilla auto-differentiation, since it reuses intermediate results from the forward pass.

Temporal loss For $\mathcal{L}_{temporal}$, note that the bottleneck for the forward pass in Eq (4) is to compute $\mathbf{A}^*_\gamma = \nabla_\Delta DTW_\gamma(\hat{\mathbf{y}}_i, \overset{*}{\mathbf{y}}_i)$, which we implement as explained for the $\mathcal{L}_{shape}$ backward pass. Regarding $\mathcal{L}_{temporal}$ backward pass, we need to compute the Hessian $\nabla^2 DTW_\gamma(\hat{\mathbf{y}}_i, \overset{*}{\mathbf{y}}_i)$. We use the method proposed in [37], based on a dynamic programming implementation that we embed in a custom Pytorch loss. Again, our back-prop implementation allows a significant speed-up compared to standard auto-differentiation (see section 4.4).

The resulting time complexity of both shape and temporal losses for forward and backward is $\mathcal{O}(k^2)$.

Discussion A variant of our approach to combine shape and temporal penalization would be to incorporate a temporal term inside our smooth $\mathcal{L}_{shape}$ function in Eq (2), *i.e.* :

$$\mathcal{L}_{DILATE^t}(\hat{\mathbf{y}}_i, \overset{*}{\mathbf{y}}_i) := -\gamma \log \left(\sum_{\mathbf{A} \in \mathcal{A}_{k,k}} \exp \left(-\frac{\left\langle \mathbf{A}, \alpha \mathbf{\Delta}(\hat{\mathbf{y}}_i, \overset{*}{\mathbf{y}}_i) + (1-\alpha)\mathbf{\Omega} \right\rangle}{\gamma} \right) \right) \tag{5}$$

We can notice that Eq (5) reduces to minimizing $\left\langle \mathbf{A}, \alpha\mathbf{\Delta}(\hat{\mathbf{y}}_i, \overset{*}{\mathbf{y}}_i) + (1-\alpha)\mathbf{\Omega} \right\rangle$ when $\gamma \to 0^+$. In this case, $\mathcal{L}_{DILATE^t}$ can recover DTW variants studied in the literature to bias the computation based on penalizing sequence misalignment, by designing specific $\mathbf{\Omega}$ matrices:

Sakoe-Chiba DTW hard band constraint [43]	$\Omega(h,j) = +\infty$ if $\lvert h-j \rvert > T$, 0 otherwise
Weighted DTW [28]	$\Omega(h,j) = f(\lvert i-j \rvert)$, f increasing function

$\mathcal{L}_{DILATE^t}$ in Eq (5) enables to train deep neural networks with a smooth loss combining shape and temporal criteria. However, $\mathcal{L}_{DILATE^t}$ presents limited capacities for disentangling the shape and temporal errors, since the optimal path is computed from both shape and temporal terms. In contrast, our $\mathcal{L}_{DILATE}$ loss in Eq (1) separates the loss into two shape and temporal misalignment components, the temporal penalization being applied to the optimal unconstrained DTW path. We verify experimentally that our $\mathcal{L}_{DILATE}$ outperforms its "tangled" version $\mathcal{L}_{DILATE^t}$ (section 4.3).

4 Experiments

4.1 Experimental setup

Datasets: To illustrate the relevance of DILATE, we carry out experiments on 3 non-stationary time series datasets from different domains (see examples in Fig 4). The multi-step evaluation consists in forecasting the future trajectory on k future time steps.
Synthetic ($k = 20$) dataset consists in predicting sudden changes (step functions) based on an input signal composed of two peaks. This controlled setup was designed to measure precisely the shape and time errors of predictions. We generate 500 times series for train, 500 for validation and 500 for test, with 40 time steps: the first 20 are the inputs, the last 20 are the targets to forecast. In each series, the input range is composed of 2 peaks of random temporal position i_1 and i_2 and random amplitude j_1 and j_2 between 0 and 1, and the target range is composed of a step of amplitude $j_2 - j_1$ and stochastic position $i_2 + (i_2 - i_1) + randint(-3, 3)$. All time series are corrupted by an additive gaussian white noise of variance 0.01.

ECG5000 ($k = 56$) dataset comes from the UCR Time Series Classification Archive [10], and is composed of 5000 electrocardiograms (ECG) (500 for training, 4500 for testing) of length 140. We take the first 84 time steps (60 %) as input and predict the last 56 steps (40 %) of each time series (same setup as in [13]).
Traffic ($k = 24$) dataset corresponds to road occupancy rates (between 0 and 1) from the California Department of Transportation (48 months from 2015-2016) measured every 1h. We work on the first univariate series of length 17544 (with the same 60/20/20 train/valid/test split as in [30]), and we train models to predict the 24 future points given the past 168 points (past week).

Network architectures and training: We perform multi-step forecasting with two kinds of neural network architectures: a fully connected network (1 layer of 128 neurons), which does not make any assumption on data structure, and a more specialized Seq2Seq model [47] with Gated Recurrent Units (GRU) [11] with 1 layer of 128 units. Each model is trained with PyTorch for a max number of 1000 epochs with Early Stopping with the ADAM optimizer. The smoothing parameter γ of DTW and TDI is set to 10^{-2}. The hyperparameter α balancing $\mathcal{L}_{shape}$ and $\mathcal{L}_{temporal}$ is determined on a validation set to get comparable DTW shape performance than the DTW_γ trained model: $\alpha = 0.5$ for Synthetic and ECG5000, and 0.8 for Traffic. Our code implementing DILATE is available on line from `https://github.com/vincent-leguen/DILATE`.

4.2 DILATE forecasting performances

We evaluate the performances of DILATE, and compare it against two strong baselines: the widely used Euclidean (MSE) loss, and the smooth DTW introduced in [13, 37]. For each experiment, we use the same neural network architecture (section 4.1), in order to isolate the impact of the training loss and to enable fair comparisons. The results are evaluated using three metrics: MSE, DTW (shape) and TDI (temporal). We perform a Student t-test with significance level 0.05 to highlight the best(s) method(s) in each experiment (averaged over 10 runs).

Overall results are presented in Table 1.

		Fully connected network (MLP)			Recurrent neural network (Seq2Seq)		
Dataset	Eval	MSE	DTW$_\gamma$ [13]	DILATE (ours)	MSE	DTW$_\gamma$ [13]	DILATE (ours)
Synth	MSE	**1.65 ± 0.14**	4.82 ± 0.40	**1.67± 0.184**	**1.10 ± 0.17**	2.31 ± 0.45	**1.21 ± 0.13**
	DTW	38.6 ± 1.28	**27.3 ± 1.37**	32.1 ± 5.33	**24.6 ± 1.20**	**22.7 ± 3.55**	**23.1 ± 2.44**
	TDI	15.3 ± 1.39	26.9 ± 4.16	**13.8 ± 0.712**	17.2 ± 1.22	20.0 ± 3.72	**14.8 ± 1.29**
ECG	MSE	**31.5 ± 1.39**	70.9 ± 37.2	37.2 ± 3.59	**21.2 ± 2.24**	75.1 ± 6.30	30.3 ± 4.10
	DTW	19.5 ± 0.159	18.4 ± 0.749	**17.7 ± 0.427**	17.8 ± 1.62	17.1 ± 0.650	**16.1 ± 0.156**
	TDI	**7.58 ± 0.192**	38.9 ± 8.76	**7.21 ± 0.886**	8.27 ± 1.03)	27.2 ± 11.1	**6.59 ± 0.786**
Traffic	MSE	**0.620 ± 0.010**	2.52 ± 0.230	1.93 ± 0.080	**0.890 ± 0.11**	2.22 ± 0.26	**1.00 ± 0.260**
	DTW	24.6 ± 0.180	**23.4 ± 5.40**	**23.1 ± 0.41**	24.6 ± 1.85	**22.6 ± 1.34**	**23.0 ± 1.62**
	TDI	**16.8 ± 0.799**	27.4 ± 5.01	**16.7 ± 0.508**	**15.4 ± 2.25**	22.3 ± 3.66	**14.4± 1.58**

Table 1: Forecasting results evaluated with MSE ($\times 100$), DTW ($\times 100$) and TDI ($\times 10$) metrics, averaged over 10 runs (mean $\pm$ standard deviation). For each experiment, best method(s) (Student t-test) in bold.

MSE comparison: DILATE outperforms MSE when evaluated on shape (DTW) in all experiments, with significant differences on 5/6 experiments. When evaluated on time (TDI), DILATE also performs better in all experiments (significant differences on 3/6 tests). Finally, DILATE is equivalent to MSE when evaluated on MSE on 3/6 experiments.

DTW$_\gamma$ [13, 37] comparison: When evaluated on shape (DTW), DILATE performs similarly to DTW$_\gamma$ (2 significant improvements, 1 significant drop and 3 equivalent performances). For time (TDI) and MSE evaluations, DILATE is significantly better than DTW$_\gamma$ in all experiments, as expected.

We display a few qualitative examples for Synthetic, ECG5000 and Traffic datasets on Fig 4 (other examples are provided in supplementary 2). We see that MSE training leads to predictions that are non-sharp, making them inadequate in presence of drops or sharp spikes. DTW$_\gamma$ leads to very sharp predictions in shape, but with a possibly large temporal misalignment. In contrast, our DILATE predicts series that have both a correct shape and precise temporal localization.

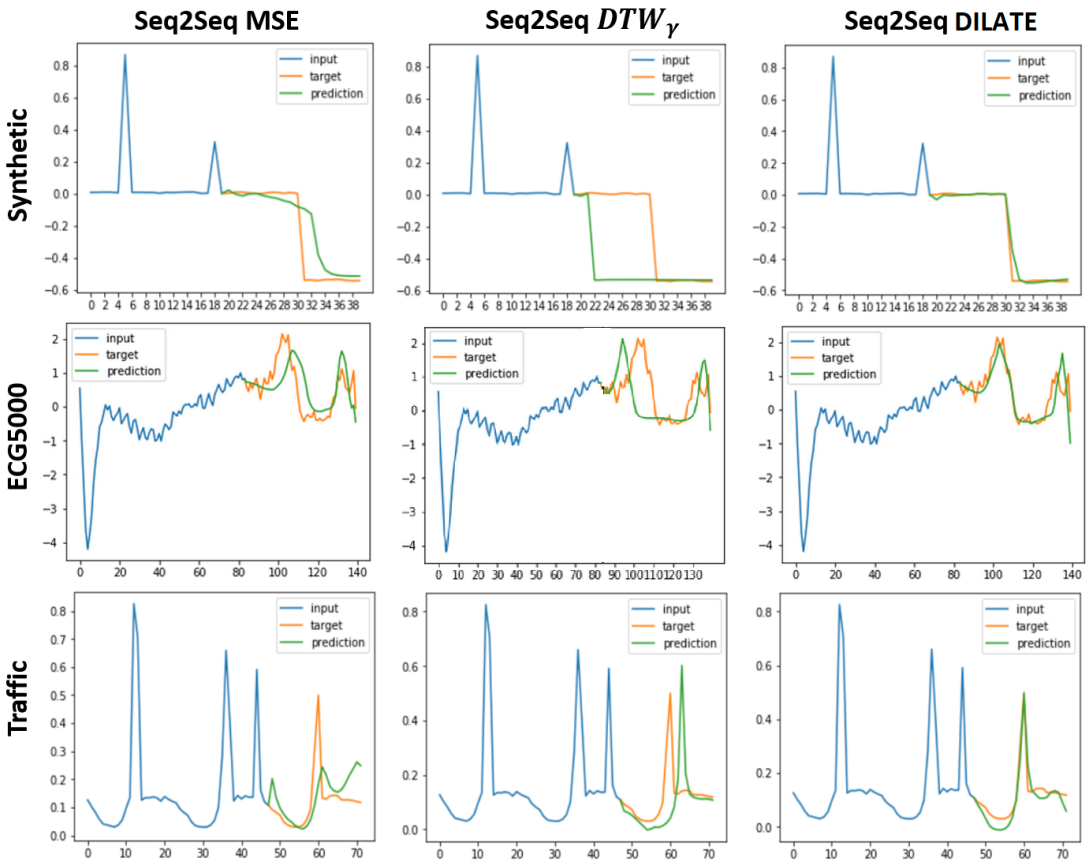

Figure 4: Qualitative forecasting results.

Evaluation with external metrics To consolidate the good behaviour of our loss function seen in Table 1, we extend the comparison using two additional (non differentiable) metrics for assessing shape and time. For shape, we compute the ramp score [52]. For time, we perform change point detection on both series and compute the Hausdorff measure between the sets of detected change points $\mathcal{T}^*$ (in the target signal) and $\hat{\mathcal{T}}$ (in the predicted signal):

$$\text{Hausdorff}(\mathcal{T}^*, \hat{\mathcal{T}}) := \max(\max_{\hat{t}\in\hat{\mathcal{T}}} \min_{t^*\in\mathcal{T}^*} |\hat{t} - t^*|, \max_{t^*\in\mathcal{T}^*} \min_{\hat{t}\in\hat{\mathcal{T}}} |\hat{t} - t^*|) \tag{6}$$

We provide more details about these external metrics in supplementary 1.1.
In Table 2, we report the comparison between Seq2Seq models trained with DILATE, DTW_γ and MSE. We see that DILATE is always better than MSE in shape (Ramp score) and equivalent to DTW_γ in 2/3 experiments. In time (Hausdorff metric), DILATE is always better or equivalent compared to MSE (and always better than DTW_γ, as expected).

		MSE	DTW_γ [13]	DILATE (ours)
Synthetic	Hausdorff	2.87 ± 0.127	3.45 ± 0.318	$\mathbf{2.70 \pm 0.166}$
	Ramp score ($\times 10$)	5.80 ± 0.104	$\mathbf{4.27 \pm 0.800}$	4.99 ± 0.460
ECG5000	Hausdorff	$\mathbf{4.32 \pm 0.505}$	6.16 ± 0.854	$\mathbf{4.23 \pm 0.414}$
	Ramp score	$\mathbf{4.84 \pm 0.240}$	$\mathbf{4.79 \pm 0.365}$	$\mathbf{4.80 \pm 0.249}$
Traffic	Hausdorff	$\mathbf{2.16 \pm 0.378}$	$\mathbf{2.29 \pm 0.329}$	$\mathbf{2.13 \pm 0.514}$
	Ramp score ($\times 10$)	6.29 ± 0.319	$\mathbf{5.78 \pm 0.404}$	$\mathbf{5.93 \pm 0.235}$

Table 2: Forecasting results of Seq2Seq evaluated with Hausdorff and Ramp Score, averaged over 10 runs (mean $\pm$ standard deviation). For each experiment, best method(s) (Student t-test) in bold.

4.3 Comparison to temporally constrained versions of DTW

In Table 3, we compare the Seq2Seq DILATE to its tangled variants Weighted DTW (DILATE^t-W) [28] and Band Constraint (DILATE^t-BC) [43] on the Synthetic dataset. We observe that DILATE performances are similar in shape for both the DTW and ramp metrics and better in time than both variants. This shows that our DILATE leads a finer disentanglement of shape and time components. Results for ECG5000 and Traffic are consistent and given in supplementary 3. We also analyze the gradient of DILATE *vs* DILATE^t-W in supplementary 3, showing that DILATE^t-W gradients are smaller at low temporal shifts, certainly explaining the superiority of our approach when evaluated with temporal metrics. Qualitative predictions are also provided in supplementary 3.

Eval loss		DILATE (ours)	DILATE^t-W [28]	DILATE^t-BC [43]
Euclidian	MSE ($\times 100$)	$\mathbf{1.21 \pm 0.130}$	1.36 ± 0.107	1.83 ± 0.163
Shape	DTW ($\times 100$)	$\mathbf{23.1 \pm 2.44}$	$\mathbf{20.5 \pm 2.49}$	$\mathbf{21.6 \pm 1.74}$
	Ramp	$\mathbf{4.99 \pm 0.460}$	$\mathbf{5.56 \pm 0.87}$	$\mathbf{5.23 \pm 0.439}$
Time	TDI ($\times 10$)	$\mathbf{14.8 \pm 1.29}$	17.8 ± 1.72	19.6 ± 1.72
	Hausdorff	$\mathbf{2.70 \pm 0.166}$	$\mathbf{2.85 \pm 0.210}$	3.30 ± 0.273

Table 3: Comparison to the tangled variants of DILATE for the Seq2Seq model on the Synthetic dataset, averaged over 10 runs (mean $\pm$ standard deviation).

4.4 DILATE Analysis

Custom backward implementation speedup: We compare in Fig 5(a) the computational time between the standard Pytorch auto-differentiation mechanism and our custom backward pass implementation (section 3.2). We plot the speedup of our implementation with respect to the prediction length k (averaged over 10 random target/prediction tuples). We notice the increasing speedup with respect to k: speedup of $\times$ 20 for 20 steps ahead and up to $\times$ 35 for 100 steps ahead predictions.

Impact of α (Fig 5(b)): When $\alpha = 1$, $\mathcal{L}_{DILATE}$ reduces to DTW_γ, with a good shape but large temporal error. When $\alpha \longrightarrow 0$, we only minimize $\mathcal{L}_{temporal}$ without any shape constraint. Both MSE and shape errors explode in this case, illustrating the fact that $\mathcal{L}_{temporal}$ is only meaningful in conjunction with $\mathcal{L}_{shape}$.

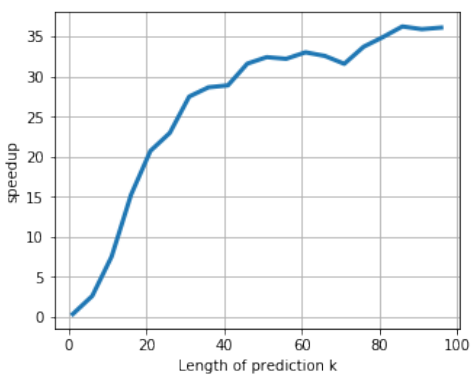

Figure 5(a): Speedup of DILATE

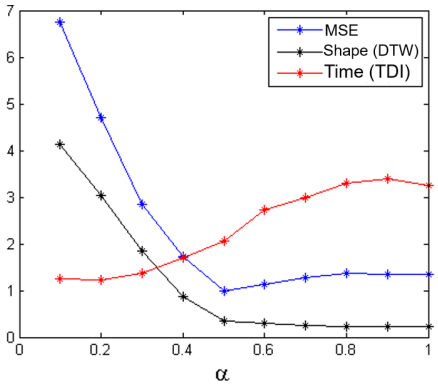

Figure 5(b): Influence of α

4.5 Comparison to state of the art time series forecasting models

Finally, we compare our Seq2Seq model trained with DILATE with two recent state-of-the-art deep architectures for time series forecasting trained with MSE: LSTNet [30] trained for one-step prediction that we apply recursively for multi-step (LSTNet-rec) ; and Tensor-Train RNN (TT-RNN) [60] trained for multi-step[2]. Results in Table 4 for the traffic dataset reveal the superiority of TT-RNN over LSTNet-rec, which shows that dedicated multi-step prediction approaches are better suited for this task. More importantly, we can observe that our Seq2Seq DILATE outperforms TT-RNN in all shape and time metrics, although it is inferior on MSE. This highlights the relevance of our DILATE loss function, which enables to reach better performances with simpler architectures.

Eval loss		LSTNet-rec [30]	TT-RNN [60, 61]	Seq2Seq DILATE
Euclidian	MSE (x100)	1.74 ± 0.11	$\mathbf{0.837 \pm 0.106}$	1.00 ± 0.260
Shape	DTW (x100)	42.0 ± 2.2	25.9 ± 1.99	$\mathbf{23.0 \pm 1.62}$
	Ramp (x10)	9.00 ± 0.577	6.71 ± 0.546	$\mathbf{5.93 \pm 0.235}$
Time	TDI (x10)	25.7 ± 4.75	17.8 ± 1.73	$\mathbf{14.4 \pm 1.58}$
	Hausdorff	$\mathbf{2.34 \pm 1.41}$	$\mathbf{2.19 \pm 0.125}$	$\mathbf{2.13 \pm 0.514}$

Table 4: Comparison with state-of-the-art forecasting architectures trained with MSE on Traffic, averaged over 10 runs (mean $\pm$ standard deviation).

5 Conclusion and future work

In this paper, we have introduced DILATE, a new differentiable loss function for training deep multi-step time series forecasting models. DILATE combines two terms for precise shape and temporal localization of non-stationary signals with sudden changes. We showed that DILATE is comparable to the standard MSE loss when evaluated on MSE, and far better when evaluated on several shape and timing metrics. DILATE compares favourably on shape and timing to state-of-the-art forecasting algorithms trained with the MSE.

For future work we intend to explore the extension of these ideas to probabilistic forecasting, for example by using bayesian deep learning [21] to compute the predictive distribution of trajectories, or by embedding the DILATE loss into a deep state space model architecture suited for probabilistic forecasting. Another interesting direction is to adapt our training scheme to relaxed supervision contexts, *e.g.* semi-supervised [42] or weakly supervised [16], in order to perform full trajectory forecasting using only categorical labels at training time (*e.g.* presence or absence of change points).

Aknowledgements We would like to thank Stéphanie Dubost, Bruno Charbonnier, Christophe Chaussin, Loïc Vallance, Lorenzo Audibert, Nicolas Paul and our anonymous reviewers for their useful feedback and discussions.

[2]We use the available Github code for both methods.

References

[1] Abubakar Abid and James Zou. Learning a warping distance from unlabeled time series using sequence autoencoders. In *Advances in Neural Information Processing Systems (NeurIPS)*, pages 10547–10555, 2018.

[2] Nguyen Hoang An and Duong Tuan Anh. Comparison of strategies for multi-step-ahead prediction of time series using neural network. In *International Conference on Advanced Computing and Applications (ACOMP)*, pages 142–149. IEEE, 2015.

[3] Yukun Bao, Tao Xiong, and Zhongyi Hu. Multi-step-ahead time series prediction using multiple-output support vector regression. *Neurocomputing*, 129:482–493, 2014.

[4] Richard Bellman. On the theory of dynamic programming. *Proceedings of the National Academy of Sciences of the United States of America*, 38(8):716, 1952.

[5] Anastasia Borovykh, Sander Bohte, and Cornelis W Oosterlee. Conditional time series forecasting with convolutional neural networks. *arXiv preprint arXiv:1703.04691*, 2017.

[6] George EP Box, Gwilym M Jenkins, Gregory C Reinsel, and Greta M Ljung. *Time series analysis: forecasting and control*. John Wiley & Sons, 2015.

[7] Rohitash Chandra, Yew-Soon Ong, and Chi-Keong Goh. Co-evolutionary multi-task learning with predictive recurrence for multi-step chaotic time series prediction. *Neurocomputing*, 243:21–34, 2017.

[8] Wei-Cheng Chang, Chun-Liang Li, Yiming Yang, and Barnabás Póczos. Kernel change-point detection with auxiliary deep generative models. In *International Conference on Learning Representations (ICLR)*, 2019.

[9] Sucheta Chauhan and Lovekesh Vig. Anomaly detection in ECG time signals via deep long short-term memory networks. In *International Conference on Data Science and Advanced Analytics (DSAA)*, pages 1–7. IEEE, 2015.

[10] Yanping Chen, Eamonn Keogh, Bing Hu, Nurjahan Begum, Anthony Bagnall, Abdullah Mueen, and Gustavo Batista. The UCR time series classification archive. 2015.

[11] Kyunghyun Cho, Bart Van Merriënboer, Caglar Gulcehre, Dzmitry Bahdanau, Fethi Bougares, Holger Schwenk, and Yoshua Bengio. Learning phrase representations using RNN encoder-decoder for statistical machine translation. *arXiv preprint arXiv:1406.1078*, 2014.

[12] Edward Choi, Mohammad Taha Bahadori, Jimeng Sun, Joshua Kulas, Andy Schuetz, and Walter Stewart. RETAIN: An interpretable predictive model for healthcare using reverse time attention mechanism. In *Advances in Neural Information Processing Systems (NIPS)*, pages 3504–3512, 2016.

[13] Marco Cuturi and Mathieu Blondel. Soft-dtw: a differentiable loss function for time-series. In *International Conference on Machine Learning (ICML)*, pages 894–903, 2017.

[14] Xiao Ding, Yue Zhang, Ting Liu, and Junwen Duan. Deep learning for event-driven stock prediction. In *International Joint Conference on Artificial Intelligence (IJCAI)*, 2015.

[15] Thibaut Durand, Nicolas Thome, and Matthieu Cord. Mantra: Minimum maximum latent structural svm for image classification and ranking. In *IEEE International Conference on Computer Vision (ICCV)*, pages 2713–2721, 2015.

[16] Thibaut Durand, Nicolas Thome, and Matthieu Cord. Exploiting negative evidence for deep latent structured models. *IEEE Transactions on Pattern Analysis and Machine Intelligence*, 41(2):337–351, 2018.

[17] James Durbin and Siem Jan Koopman. *Time series analysis by state space methods*. Oxford university press, 2012.

[18] Anthony Florita, Bri-Mathias Hodge, and Kirsten Orwig. Identifying wind and solar ramping events. In *2013 IEEE Green Technologies Conference (GreenTech)*, pages 147–152. IEEE, 2013.

[19] Ian Fox, Lynn Ang, Mamta Jaiswal, Rodica Pop-Busui, and Jenna Wiens. Deep multi-output forecasting: Learning to accurately predict blood glucose trajectories. In *ACM SIGKDD International Conference on Knowledge Discovery & Data Mining*, pages 1387–1395. ACM, 2018.

[20] Laura Frías-Paredes, Fermín Mallor, Martín Gastón-Romeo, and Teresa León. Assessing energy forecasting inaccuracy by simultaneously considering temporal and absolute errors. *Energy Conversion and Management*, 142:533–546, 2017.

[21] Yarin Gal and Zoubin Ghahramani. Dropout as a bayesian approximation: Representing model uncertainty in deep learning. In *International Conference on Machine Learning (ICML)*, pages 1050–1059, 2016.

[22] Damien Garreau, Sylvain Arlot, et al. Consistent change-point detection with kernels. *Electronic Journal of Statistics*, 12(2):4440–4486, 2018.

[23] Amir Ghaderi, Borhan M Sanandaji, and Faezeh Ghaderi. Deep forecast: Deep learning-based spatio-temporal forecasting. In *ICML Time Series Workshop*, 2017.

[24] Agathe Girard and Carl Edward Rasmussen. Multiple-step ahead prediction for non linear dynamic systems - a gaussian process treatment with propagation of the uncertainty. In *Advances in neural information processing systems (NIPS)*, volume 15, pages 529–536, 2002.

[25] Sepp Hochreiter and Jürgen Schmidhuber. Long short-term memory. *Neural Computing*, 9(8):1735–1780, November 1997.

[26] Shamina Hussein, Rohitash Chandra, and Anuraganand Sharma. Multi-step-ahead chaotic time series prediction using coevolutionary recurrent neural networks. In *IEEE Congress on Evolutionary Computation (CEC)*, pages 3084–3091. IEEE, 2016.

[27] Rob Hyndman, Anne B Koehler, J Keith Ord, and Ralph D Snyder. *Forecasting with exponential smoothing: the state space approach*. Springer Science & Business Media, 2008.

[28] Young-Seon Jeong, Myong K Jeong, and Olufemi A Omitaomu. Weighted dynamic time warping for time series classification. *Pattern Recognition*, 44:2231–2240, 2011.

[29] Vitaly Kuznetsov and Zelda Mariet. Foundations of sequence-to-sequence modeling for time series. In *International Conference on Artificial Intelligence and Statistics (AISTATS)*, 2019.

[30] Guokun Lai, Wei-Cheng Chang, Yiming Yang, and Hanxiao Liu. Modeling long-and short-term temporal patterns with deep neural networks. In *ACM SIGIR Conference on Research & Development in Information Retrieval*, pages 95–104. ACM, 2018.

[31] Nikolay Laptev, Jason Yosinski, Li Erran Li, and Slawek Smyl. Time-series extreme event forecasting with neural networks at Uber. In *International Conference on Machine Learning (ICML)*, number 34, pages 1–5, 2017.

[32] Shiyang Li, Xiaoyong Jin, Yao Xuan, Xiyou Zhou, Wenhu Chen, Wang Yu-Xiang, and Yan Xifeng. Enhancing the locality and breaking the memory bottleneck of transformer on time series forecasting. In *Advances in neural information processing systems (NeurIPS)*, 2019.

[33] Shuang Li, Yao Xie, Hanjun Dai, and Le Song. M-statistic for kernel change-point detection. In *Advances in Neural Information Processing Systems (NIPS)*, pages 3366–3374, 2015.

[34] Yaguang Li, Rose Yu, Cyrus Shahabi, and Yan Liu. Diffusion convolutional recurrent neural network: Data-driven traffic forecasting. In *International Conference on Learning Representations (ICLR)*, 2018.

[35] Yisheng Lv, Yanjie Duan, Wenwen Kang, Zhengxi Li, and Fei-Yue Wang. Traffic flow prediction with big data: a deep learning approach. *IEEE Transactions on Intelligent Transportation Systems*, 16(2):865–873, 2015.

[36] Shamsul Masum, Ying Liu, and John Chiverton. Multi-step time series forecasting of electric load using machine learning models. In *International Conference on Artificial Intelligence and Soft Computing*, pages 148–159. Springer, 2018.

[37] Arthur Mensch and Mathieu Blondel. Differentiable dynamic programming for structured prediction and attention. *International Conference on Machine Learning (ICML)*, 2018.

[38] Sebastian Nowozin. Optimal decisions from probabilistic models: the intersection-over-union case. In *IEEE Conference on Computer Vision and Pattern Recognition (CVPR)*, pages 548–555, 2014.

[39] Yao Qin, Dongjin Song, Haifeng Cheng, Wei Cheng, Guofei Jiang, and Garrison W Cottrell. A dual-stage attention-based recurrent neural network for time series prediction. In *International Joint Conference on Artificial Intelligence (IJCAI)*, pages 2627–2633. AAAI Press, 2017.

[40] Syama Sundar Rangapuram, Matthias W Seeger, Jan Gasthaus, Lorenzo Stella, Yuyang Wang, and Tim Januschowski. Deep state space models for time series forecasting. In *Advances in Neural Information Processing Systems (NeurIPS)*, pages 7785–7794, 2018.

[41] François Rivest and Richard Kohar. A new timing error cost function for binary time series prediction. *IEEE transactions on neural networks and learning systems*, 2019.

[42] Thomas Robert, Nicolas Thome, and Matthieu Cord. Hybridnet: Classification and reconstruction cooperation for semi-supervised learning. In *European Conference on Computer Vision (ECCV)*, pages 153–169, 2018.

[43] Hiroaki Sakoe and Seibi Chiba. Dynamic programming algorithm optimization for spoken word recognition. *Readings in speech recognition*, 159:224, 1990.

[44] David Salinas, Valentin Flunkert, and Jan Gasthaus. DeepAR: Probabilistic forecasting with autoregressive recurrent networks. In *International Conference on Machine Learning (ICML)*, 2017.

[45] Matthias W Seeger, David Salinas, and Valentin Flunkert. Bayesian intermittent demand forecasting for large inventories. In *Advances in Neural Information Processing Systems (NIPS)*, pages 4646–4654, 2016.

[46] Rajat Sen, Yu Hsiang-Fu, and Dhillon Inderjit. Think globally, act locally: a deep neural network approach to high dimensional time series forecasting. In *Advances in Neural Information Processing Systems (NeurIPS)*, 2019.

[47] Ilya Sutskever, Oriol Vinyals, and Quoc V Le. Sequence to sequence learning with neural networks. In *Advances in neural information processing systems (NIPS)*, pages 3104–3112, 2014.

[48] Souhaib Ben Taieb and Amir F Atiya. A bias and variance analysis for multistep-ahead time series forecasting. *IEEE Transactions on Neural Networks and Learning Systems*, 27(1):62–76, 2016.

[49] Souhaib Ben Taieb, Gianluca Bontempi, Amir F Atiya, and Antti Sorjamaa. A review and comparison of strategies for multi-step ahead time series forecasting based on the NN5 forecasting competition. *Expert systems with applications*, 39(8):7067–7083, 2012.

[50] Yunzhe Tao, Lin Ma, Weizhong Zhang, Jian Liu, Wei Liu, and Qiang Du. Hierarchical attention-based recurrent highway networks for time series prediction. *arXiv preprint arXiv:1806.00685*, 2018.

[51] Charles Truong, Laurent Oudre, and Nicolas Vayatis. Supervised kernel change point detection with partial annotations. In *International Conference on Acoustics, Speech and Signal Processing (ICASSP)*, pages 3147–3151. IEEE, 2019.

[52] Loïc Vallance, Bruno Charbonnier, Nicolas Paul, Stéphanie Dubost, and Philippe Blanc. Towards a standardized procedure to assess solar forecast accuracy: A new ramp and time alignment metric. *Solar Energy*, 150:408–422, 2017.

[53] Aäron Van Den Oord, Sander Dieleman, Heiga Zen, Karen Simonyan, Oriol Vinyals, Alex Graves, Nal Kalchbrenner, Andrew W Senior, and Koray Kavukcuoglu. WaveNet: A generative model for raw audio. *arXiv preprint arXiv:1609.03499*, 2016.

[54] Ashish Vaswani, Noam Shazeer, Niki Parmar, Jakob Uszkoreit, Llion Jones, Aidan N Gomez, Łukasz Kaiser, and Illia Polosukhin. Attention is all you need. In *Advances in neural information processing systems (NIPS)*, pages 5998–6008, 2017.

[55] Arun Venkatraman, Martial Hebert, and J Andrew Bagnell. Improving multi-step prediction of learned time series models. In *Twenty-Ninth AAAI Conference on Artificial Intelligence*, 2015.

[56] Yuyang Wang, Alex Smola, Danielle Maddix, Jan Gasthaus, Dean Foster, and Tim Januschowski. Deep factors for forecasting. In *International Conference on Machine Learning (ICML)*, pages 6607–6617, 2019.

[57] Ruofeng Wen, Kari Torkkola, Balakrishnan Narayanaswamy, and Dhruv Madeka. A multi-horizon quantile recurrent forecaster. *NIPS Time Series Workshop*, 2017.

[58] Hsiang-Fu Yu, Nikhil Rao, and Inderjit S Dhillon. Temporal regularized matrix factorization for high-dimensional time series prediction. In *Advances in neural information processing systems (NIPS)*, pages 847–855, 2016.

[59] Jiaqian Yu and Matthew B Blaschko. The lovász hinge: A novel convex surrogate for submodular losses. *IEEE Transactions on Pattern Analysis and Machine Intelligence*, 2018.

[60] Rose Yu, Stephan Zheng, Anima Anandkumar, and Yisong Yue. Long-term forecasting using tensor-train RNNs. *arXiv preprint arXiv:1711.00073*, 2017.

[61] Rose Yu, Stephan Zheng, and Yan Liu. Learning chaotic dynamics using tensor recurrent neural networks. In *ICML Workshop on Deep Structured Prediction*, volume 17, 2017.

[62] Yisong Yue, Thomas Finley, Filip Radlinski, and Thorsten Joachims. A support vector method for optimizing average precision. In *ACM SIGIR conference on Research and development in information retrieval*, pages 271–278. ACM, 2007.

[63] Jian Zheng, Cencen Xu, Ziang Zhang, and Xiaohua Li. Electric load forecasting in smart grids using long-short-term-memory based recurrent neural network. In *51st Annual Conference on Information Sciences and Systems (CISS)*, pages 1–6. IEEE, 2017.